STEALTH CRATERS IN THE NORTHERN LOWLANDS OF MARS: EVIDENCE FOR A BURIED EARLY-HESPERIAN-AGED UNIT. ***M. A. Kreslavsky***[1,2] and ***J. W. Head III***[2], [1]Kharkov Astronomical Observatory, 35 Sumska, Kharkov, 61022, Ukraine, misha@mare.geo.brown.edu, [2]Dept. Geol. Sci., Brown University, Providence RI 02912-1864, USA, James_Head_III@Brown.edu.

Introduction: The vast northern lowlands of Mars are characterized by a general smoothness of topography and a paucity of sharply-defined geological features in mid-resolution images. The latter is partly due to poor observation conditions (persistent haze, polar hood) and extensive coverage of the surface with various surficial deposits. MGS MOLA topographic data [1] have high vertical accuracy and spatial resolution of ~3 km. These allowed us to study tens-kilometer-scale features poorly seen in the images. This work is focused on a population of degraded craters. An accompanied abstract [2] is devoted to ridges.

Detrended topography map: To take advantage of the high accuracy of MOLA topographic data we removed the regional topography from the topographic maps. For each element of gridded topography, we subtracted the median elevation calculated in the 50-km vicinity of the element from the elevation of the element. In this way we obtain the detrended topography map (a small part of it is shown in **Fig. 1**; brighter shades denote locally higher elevations).

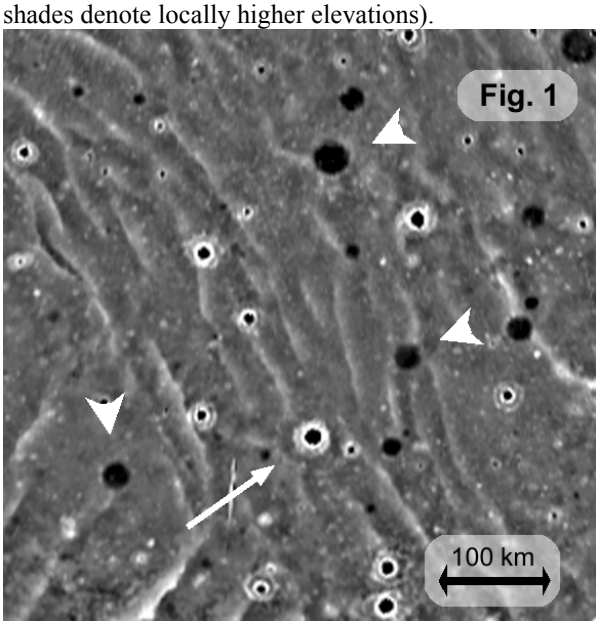

Survey of stealth craters: There are many smooth shallow flat-floored circular depressions in the northern lowlands (like those shown by the wide arrows in **Fig. 1**). Their perfect circular form and apparently random scattering around the surface indicate their impact origin. We called such objects stealth craters. Some of them can be recognized in Viking low-resolution mosaics, while many of them are too smooth to be visible in the images. The stealth craters clearly differ from real, fresh craters: all fresh craters have distinctive rims and ejecta patterns (e.g., thin arrow in **Fig. 1)**.

We identified and marked all stealth craters in the northern lowlands. We calculated the diameter of each stealth crater as the diameter of a circle having the same area as the marked depression. The largest stealth crater is 169 km in diameter; the second largest is 75 km. The smallest identified stealth craters are about 6 km. Identification of stealth craters smaller than 10-15 km is not reliable, and the diameter estimates are not accurate. For further analysis we used only craters larger than 16 km. There are 140 such objects. Their cumulative size-frequency distribution is shown in **Fig. 2** (thin line), the incremental distribution for a set of conventional diameter bins is shown in **Fig. 3** (hashed bars).

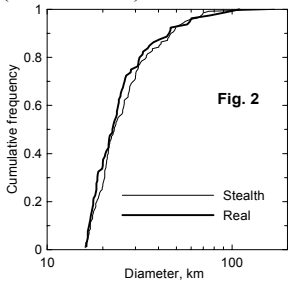

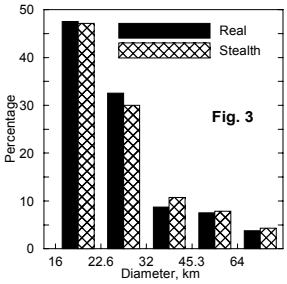

Stealth craters appear only within the boundaries of the Vastitas Borealis Formation (Hv) [3-5]. Probably these craters were formed in a substrate before or during the Hv emplacement and then were heavily modified and obscured by Hv material.

Comparison with fresh craters: Straightforward use of available data on fresh craters for these purposes is impossible, because our diameter measure is different from that commonly used. Rim crest-to-rim crest diameter cannot be applied to stealth craters because they do not have distinctive rims. Strictly speaking, we do not know the details of the crater modification process; hence, we cannot unambiguously tie our measured diameters to any morphometric characteristics of pristine craters. We proceed by making the reasonable assumption that the size of a stealth crater is equal to the size of inner depression of a pristine crater. We identified all real (fresh) craters within the Hv outline and measured their sizes in the same manner as we did for the stealth craters. The total number of real craters larger than 16 km is 80. Their size-frequency distributions are shown in **Fig. 2** (bold line) and **3** (solid bars).

Morphometry: We measured the depth of the craters as the difference between the elevation of the surroundings and the elevation of the crater floor. The elevation of the crater floor was calculated as the median elevation within a circle around the crater center with the diameter twice smaller than the crater diameter. We checked that for the distinctive, non-stealth craters, the elevation calculated in this way usually reflects the elevation of the floor rather then the elevation of the central peak or peak ring. The elevation of surroundings was calculated as the median elevation within a ring between 4 and 4.25 crater diameters from the center. For the real craters, such a ring is usually outside the ejecta. The measured depth is plotted against crater size in **Fig. 4**. Several pedestal craters have negative depths: their floor is higher than their surroundings. The depth of real craters is widely scattered, though large craters are generally deeper. The depth of the stealth craters is scattered around 100 m, and no dependence of the depth on crater size is observed. Only two stealth craters are deeper than 200 m.

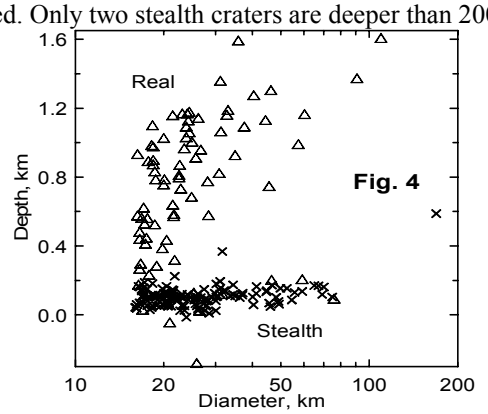

The very shallow nature of the stealth craters is consistent with their extensive erosion and infill after their formation on an underlying unit. The contrast in crater depths between these two populations suggests that the stealth craters underwent modification and shallowing during Late Hesperian, most likely coincident with the emplacement of Hv.

Age estimation: The size-frequency distribution of the stealth craters turned out to be remarkably similar to that of real craters (**Fig. 2, 3**). It is probable that we see almost all craters formed on the substrate before the emplacement of Hv; otherwise, we would expect a noticeable relative paucity of small stealth craters. Thus we can use the total number of stealth and fresh craters (220, which gives the density of 13.0 per 10^6 km^2) to estimate the age of the **substrate**. It cannot be done directly because (1) for 16-km crater density the Martian chronology [6] is established for the Noachian only, and (2) our size measure is biased in comparison to that used for the chronology. We tied our data to the chronology by two principally different ways, which gave the same result: the substrate is Early Hesperian.

Relative density. For smaller craters, the Hesperian spans a factor of three in crater density [6]. We assume that the density of craters >16 km changes in approximately the same way from the lower to the upper boundary of the Hesperian. The density of fresh craters in Hv is 2.75 times lower than the density of fresh + stealth craters. Thus, if we postulate Hv to be Upper Hesperian and close to the Amazonian boundary, the substrate will be Lower Hesperian and close to the Noachian boundary.

Absolute density. The crater catalog [7] kindly provided to us by N. Barlow contains 167 craters larger than 16 km for the rim-to-rim diameter within the Hv outline. Among them, 26 craters do not have noticeable rims or ejecta patterns in the detrended topography. We interpret that the rest 167-26=141 craters in the catalog postdate Hv. This number is 1.76 times greater than our number of fresh craters. This factor can be used to bring our crater densities to the commonly used system. Applying this factor to our density of fresh + stealth craters, we obtain 23 per 10^6 km^2, just a little less than the Hesperian/Noachian boundary defined in [6] at 25 per 10^6 km^2.

Interaction of ridges and craters: There are several sites where the ridge pattern [2] "knows" about the existence of a *stealth* crater (**Fig. 1**, wide arrows) similarly to that observed in [8] for wrinkle ridges and craters in the Coprates region. This shows that ridge formation occurred (or continued) some time after the deposit of the substrate material. The observations do not provide good constraints on this time; however, it is clear that it could be a measurable part of the Hesperian. There are no convincing examples of ridges postdating fresh craters. We found two sites where ridges might be thought to be influenced by real craters, but these examples are ambiguous (e.g., ridges to S and W of the crater marked with the narrow arrow in **Fig. 1**). There are numerous examples where ridges are covered and obscured by crater ejecta (e.g. NW-SE trending ridges at the same crater, **Fig. 1**). This suggests that wrinkle ridge formation had ceased, although the exact duration and time of cessation is unknown.

References: [1] Smith D. E. et al. (1999) *Science 284* 1495. [2] Head J. W. and Kreslavsky M. A. (2001) *LPS XXXII,* this volume; Also Head J. W. and Kreslavsky M. A. (2001) *JGR*, submitted. [3] Scott D. H. and Tanaka K. L. (1986) USGS map I-1802-A. [4] Tanaka K. L. and Scott D. H. (1987) USGS map I-1802-C. [5] Greeley R. and Guest J. E. (1987) USGS map I-1802-B. [6] Tanaka K. L. (1986) *Proc. LPSC XVII, JGR 91*, E139. [7] Barlow N. G. (1988) *Icarus 75* 285. [8] Allemand P. and Thomas P. G. (1995) *JGR 100*, 3251.